

Initial conditions of heavy ion collisions and small x

T. Lappi^{a,b}

^a*Department of Physics P.O. Box 35, 40014 University of Jyväskylä, Finland*

^b*Institut de Physique Théorique, Bât. 774, CEA/DSM/Saclay, 91191 Gif-sur-Yvette Cedex, France*

Abstract

The Color Glass Condensate (CGC), describing the physics of the nonlinear gluonic interactions of QCD at high energy, provides a consistent first-principles framework to understand the initial conditions of heavy ion collisions. This talk reviews some aspects of the initial conditions at RHIC, and discusses implications for LHC heavy ion phenomenology. The CGC provides a way to compute bulk particle production and understand recent experimental observations of long range rapidity correlations in terms of the classical glasma field in the early stages of the collision.

Key words:

PACS: 24.85.+p, 25.75.-q, 12.38.Mh

1. Introduction

The Relativistic Heavy Ion Collider (RHIC) at Brookhaven has been in operation since 2000 and has produced a wealth of experimental results. The combination of new theoretical developments with these observations has taught us a lot about different aspects of the collision process and given much insight into what we can expect from the LHC heavy ion programme. The focus of this talk is on the initial stages of the collision process and how it can be understood from first principles knowledge of the high energy wavefunction of a hadron or a nucleus. We shall first discuss the Color Glass Condensate (CGC, for reviews see [1]) picture of the wavefunction and how it leads to the Glasma [2] field configurations in the initial nonequilibrium stage of the collision. We then move on, in Sec. 2, to discuss the predictions for the total multiplicities. Section 3 deals with more detailed aspects of the collision geometry and Sec. 4 with some more recent ideas of Glasma physics.

The central rapidity region in high energy collisions originates from the interaction of the “slow” small x degrees of freedom, predominantly gluons, in the wavefunctions of the incoming hadrons or nuclei. At large energies these gluons form a dense system that is characterized by a *saturation scale* Q_s . The degrees of freedom with $p_T \lesssim Q_s$

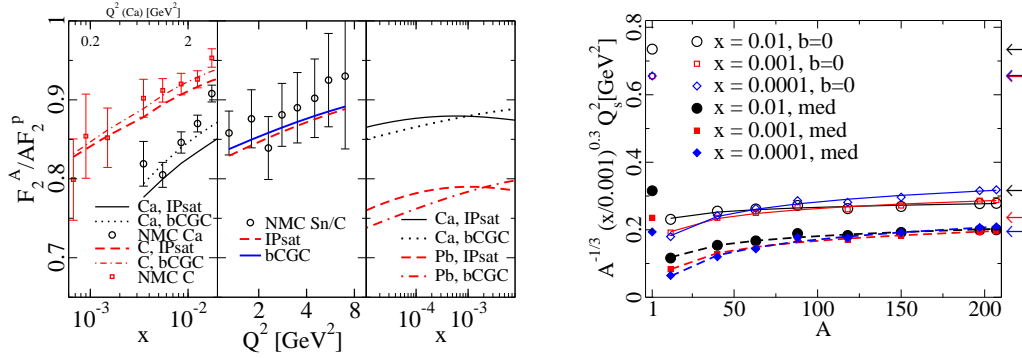


Fig. 1. Left: comparison of CGC-based fits to HERA data (IPsat and bCGC models) with the existing eA data. Right: Values of the saturation scale in nuclei. For details see [3].

are fully nonlinear Yang-Mills fields with large field strength $A_\mu \sim 1/g$ and occupation numbers $\sim 1/\alpha_s$, they can therefore be understood as classical fields radiated from the large x partons. Note that while this description is inherently nonperturbative, it is still based on a weak coupling argument, because the classical approximation requires $1/\alpha_s$ to be large and therefore $Q_s \gg \Lambda_{\text{QCD}}$. A “pocket formula” [3] for estimating the energy and nuclear dependence of the saturation scale is $Q_s^2 \sim A^{1/3} x^{-0.3}$: nonlinear high gluon density effects are enhanced by going to small x and large nuclei. Ideally one would like to study the physics of the CGC at the Electron Ion Collider [4], but already based on fits to HERA data and simple nuclear geometry we have a relatively good idea of the magnitude of Q_s at RHIC energies as shown in Fig. 1. The CGC is a systematic effective theory (effective because the large x part of the wavefunction is integrated out) formulation of these degrees of freedom, and the term glasma refers to the coherent, classical field configuration resulting from the collision of two such objects CGC.

2. Bulk gluon production

In order to compute particle production in the Glasma one starts with the following setup [5]. The valence-like degrees of freedom of the two nuclei are represented by two classical color currents that are, because of their large longitudinal momenta (p^\pm) well localized on the light cone (in the variables conjugate to p^\pm , namely x^\mp): $J^\pm \sim \delta(x^\mp)$. These then generate the classical field that one wants to find. Working in light cone gauge (actually $A_\tau = 0$ -gauge for the two nucleus problem), the field in the region of spacetime causally connected to only one of the nuclei is a transverse pure gauge, independently for each of the two nuclei. These pure gauge fields then give the initial condition on the future light cone ($\tau = \sqrt{2x^+x^-} = 0$) for the nontrivial gauge field after the collision. The spacetime structure of these fields is illustrated in Fig. 2. The field inside the future light cone can then be computed either numerically [6] or analytically in different

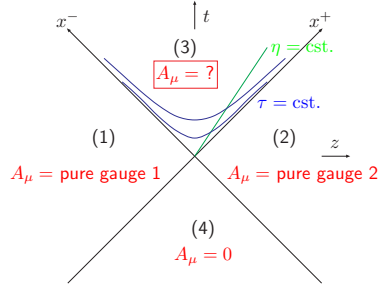


Fig. 2. Classical field configurations.

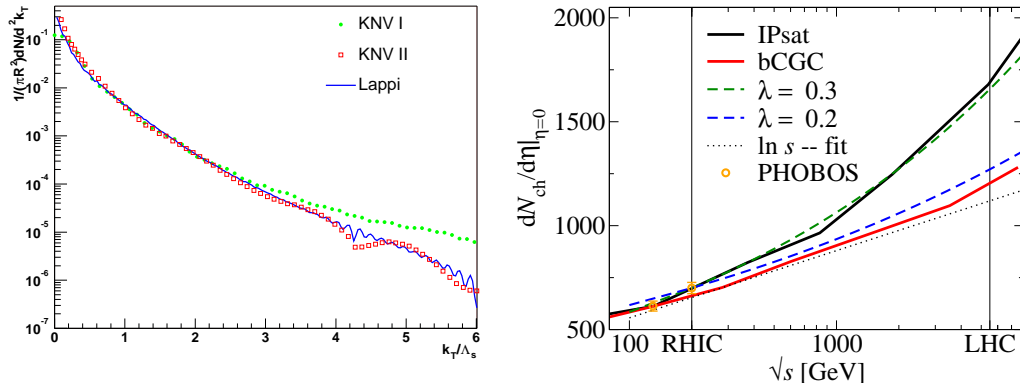


Fig. 3. Left: gluon spectrum from CYM calculations [6]. Right: energy dependence of the multiplicity in central collisions based on two fits to HERA data [10].

approximations (see e.g. [7] for recent work). The obtained result is then averaged over the configurations of the sources J^μ with a distribution $W_y[J^\mu]$ that includes the non-perturbative knowledge of the large x degrees of freedom. The resulting fields are then decomposed into Fourier modes to get the gluon spectrum, see Fig. 3. This is the method that we will refer to as Classical Yang-Mills (CYM) calculations. Note that the average over configurations is a classical average over a probabilistic distribution. This is guaranteed by a theorem [8] ensuring the factorization of leading logarithmic corrections to gluon production into the quantum evolution of $W_y[J^\mu]$, analogously to the way leading logarithms of Q^2 are factorized into DGLAP-evolved parton distribution functions.

In the limit when either one or both of the color sources are dilute (the “pp” and “pA” cases), the CYM calculation can be done analytically and reduces to a factorized form in terms of a convolution of unintegrated parton distributions that can include saturation effects. Although this approach (known as “KLN” after the authors of [9]) is not strictly valid for the collision of two dense systems, it does have the advantage of offering some analytical insight and making it easier to incorporate large- x ingredients into the calculation.

The CYM calculations [6] of gluon production paint a fairly consistent picture of gluon production at RHIC. The estimated value $Q_s \approx 1.2$ GeV from HERA data [3] (corresponding to the MV model parameter $g^2\mu \approx 2.1$ GeV [11]) leads to $\frac{dN}{dy} \approx 1100$ gluons in the initial stage. Assuming a rapid thermalization and nearly ideal hydrodynamical evolution this is consistent with the observed ~ 700 charged (~ 1100 total) particles produced in a unit of rapidity in central collisions.

The gluon multiplicity is, across different parametrizations to a very good approximation proportional to $\pi R_A^2 Q_s^2/\alpha_s$. Thus the predictions for LHC collisions depend mostly on the energy dependence of Q_s . On this front there is perhaps more uncertainty than is generally acknowledged, the estimates for $\lambda = d \ln Q_s^2 / d \ln 1/x$ varying between $\lambda = 0.29$ [12] and $\lambda = 0.18$ [13] in fixed coupling fits to HERA data, with a running coupling solution of the BK equation giving something in between these values [14]. This dominates the uncertainty in predictions for the LHC multiplicity (see Fig. 3).

The RHIC collision energy is still too slow to clearly see any saturation effects in the rapidity dependence of the multiplicity around $y = 0$. A simple estimate for the effects

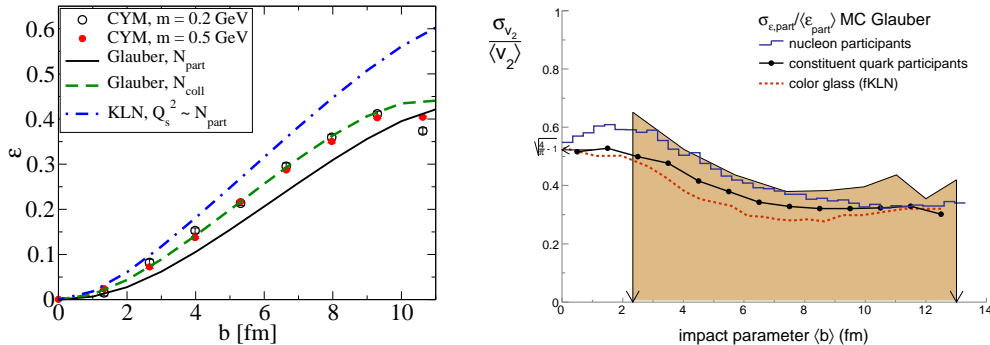


Fig. 4. Left: initial eccentricity from CYM [15] (“KLN” is the result of Ref. [16]). Right: eccentricity fluctuations from STAR compared to the “fKLN” model [17].

of large x physics, such as momentum conservation, is to consider the typical $(1-x)^4$ -dependence of gluon distributions at large x . Inserting $x = e^{\pm y} \langle p_{\perp} \rangle / \sqrt{s}$ leads to the estimate $\Delta y \sim \sqrt{8\sqrt{s} / \langle p_{\perp} \rangle}$ for the rapidity scale at which the large x effects contribute to the rapidity distribution around $y = 0$, with $\Delta y \sim 4$ RHIC and $\Delta y \sim 19$ at LHC. The large x contribution is an effect of order 1 at this scale, whereas small x evolution can be expected to give a much smaller effect [18] at a rapidity scale $\Delta y \sim 1/\alpha_s \sim 3$. Only at the LHC the large x effects will be mostly absent around midrapidity and one has a good possibility of seeing CGC effects in the rapidity dependence of the multiplicity.

3. Geometry

The basic features (such as the mostly N_{part} scaling) of the centrality dependence of particle multiplicities are mostly straightforward consequences of geometry and the proportionality of the multiplicity to Q_s^2 ; they are successfully reproduced by both KLN and CYM calculations [9,15,17], see Fig. 4. A striking signal of collective behavior of the matter produced at RHIC is elliptic flow. Comparing hydrodynamical calculations with flow is a way to address fundamental observable properties of the medium, such as viscosity, but this comparison requires understanding of the initial conditions of the hydrodynamical evolution, particularly the initial eccentricity for elliptic flow. The original general consensus some years ago was that ideal hydrodynamics is in good agreement with the experimental data, but this claim has been questioned recently after it was argued using a KLN-type calculation [16] that CGC results in a larger initial eccentricity, leaving more room for viscosity in the hydrodynamical evolution. It was subsequently pointed out in Ref. [15] that this claim of a higher initial eccentricity was caused partly by the unphysical nonuniversal saturation scale used in the KLN calculation. The result of the CYM calculation [15], later confirmed in a modified KLN framework [19] is that when the nonuniversality effect is corrected for, the CGC eccentricity is indeed higher (closer to the energy density scaling with the number of collisions) than the traditional initial conditions used in hydrodynamical calculations (with N_{part} scaling), but not as large as in Ref. [16]. The difference is illustrated in Fig. 4. A much more detailed probe of our understanding of the initial geometry is provided by fluctuations [20] in the elliptic flow, for some early work on the subject see Ref. [17].

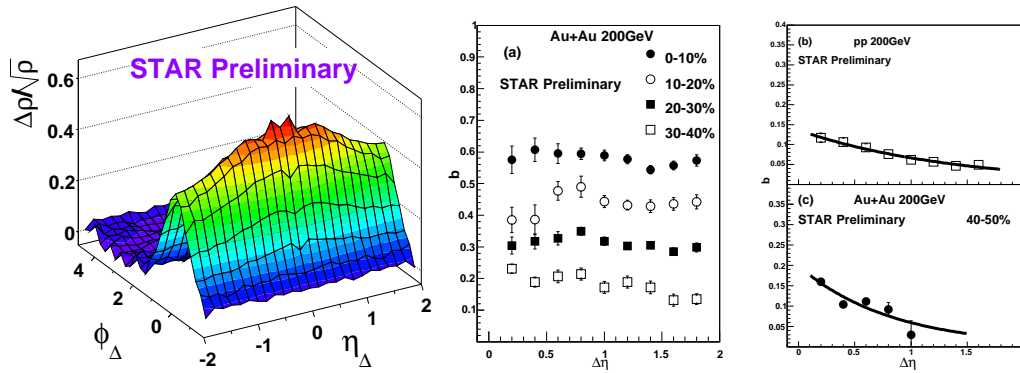


Fig. 5. Left: two particle correlation from STAR, showing the “ridge” structure elongated in pseudorapidity. Right: Long range correlations in multiplicity: $b = (\langle N_F N_B \rangle - \langle N_F \rangle \langle N_B \rangle) / (\langle N_F^2 \rangle - \langle N_F \rangle^2)$, where F and B are pseudorapidity bins separated by $\Delta\eta$ [21].

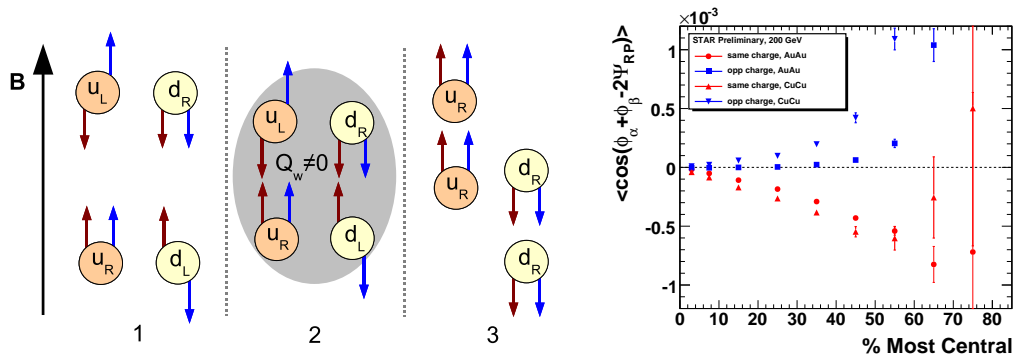


Fig. 6. Left: chiral magnetic effect: the blue (right) arrow is the spin (aligned with B) and the red (left) the momentum, the evolution of the system through a configuration of nonzero Chern-Simons charge generates a net chirality that aligns the momenta with the spin and thus the external magnetic field, i.e. the reaction plane. Right: parity violating correlation between reaction plane and momentum [22].

4. Glasma physics

Correlations over large distances in rapidity must, by causality, originate from the earliest times in the collision process, and are thus sensitive to the properties of the glasma phase of the collision. Examples of such phenomena are the “ridge” and long range correlations in multiplicity [21] (see Fig. 5). The boost invariant nature of the Glasma fields naturally leads to this kind of a correlation, and deviations from it should be calculable from the high energy evolution governing the rapidity dependence [23]

Another remarkable phenomenon that is possible in the Glasma field configuration is the generation of a large Chern-Simons charge and thus parity violation [24] due to the nonperturbatively large field configuration. Through the so called “chiral magnetic effect” (see Fig. 6) this can manifest itself in a parity violating correlation between the electric dipole moment (or momentum anisotropy between negative and positive charges; a vector) and the reaction plane (the positive charges of the ions generate a magnetic field perpendicular to the reaction plane; a pseudovector). There are some preliminary

indications in the data for such a nonzero value for such an observable [22].

In conclusion, RHIC data has given much quantitative insight into the small x physics of the initial conditions, both on a quantitative level and by revealing new qualitative phenomena. These form a good basis for LHC predictions, better than the theoretical situation was before the start of RHIC operations. Given the much higher energy of the LHC there are, however, also qualitatively new phenomena in the physics of the Glasma that will only open up to experimental study at the LHC.

The author is supported by the Academy of Finland, contract 126604.

References

- [1] E. Iancu and R. Venugopalan, arXiv:hep-ph/0303204; H. Weigert, Prog. Part. Nucl. Phys. **55**, 461 (2005), [arXiv:hep-ph/0501087].
- [2] T. Lappi and L. McLerran, Nucl. Phys. **A772**, 200 (2006), [arXiv:hep-ph/0602189].
- [3] H. Kowalski, T. Lappi and R. Venugopalan, Phys. Rev. Lett. **100**, 022303 (2008), [arXiv:0705.3047 [hep-ph]].
- [4] A. Deshpande, R. Milner, R. Venugopalan and W. Vogelsang, Ann. Rev. Nucl. Part. Sci. **55**, 165 (2005), [arXiv:hep-ph/0506148].
- [5] A. Kovner, L. D. McLerran and H. Weigert, Phys. Rev. **D52**, 3809 (1995), [arXiv:hep-ph/9505320].
- [6] A. Krasnitz, Y. Nara and R. Venugopalan, Phys. Rev. Lett. **87**, 192302 (2001), [arXiv:hep-ph/0108092]; T. Lappi, Phys. Rev. **C67**, 054903 (2003), [arXiv:hep-ph/0303076]; A. Krasnitz, Y. Nara and R. Venugopalan, Nucl. Phys. **A727**, 427 (2003), [arXiv:hep-ph/0305112].
- [7] J.-P. Blaizot and Y. Mehtar-Tani, arXiv:0806.1422 [hep-ph].
- [8] F. Gelis, T. Lappi and R. Venugopalan, Phys. Rev. **D78**, 054019 (2008), [arXiv:0804.2630 [hep-ph]]; F. Gelis, T. Lappi and R. Venugopalan, Phys. Rev. **D78**, 054020 (2008), [arXiv:0807.1306 [hep-ph]].
- [9] D. Kharzeev and M. Nardi, Phys. Lett. **B507**, 121 (2001), [arXiv:nucl-th/0012025]; D. Kharzeev and E. Levin, Phys. Lett. **B523**, 79 (2001), [arXiv:nucl-th/0108006].
- [10] T. Lappi, J. Phys. **G35**, 104052 (2008), [arXiv:0804.2338 [hep-ph]].
- [11] T. Lappi, Eur. Phys. J. **C55**, 285 (2008), [arXiv:0711.3039 [hep-ph]].
- [12] K. Golec-Biernat and M. Wusthoff, Phys. Rev. **D59**, 014017 (1999), [arXiv:hep-ph/9807513].
- [13] H. Kowalski, L. Motyka and G. Watt, Phys. Rev. **D74**, 074016 (2006), [arXiv:hep-ph/0606272].
- [14] J. L. Albacete, Phys. Rev. Lett. **99**, 262301 (2007), [arXiv:0707.2545 [hep-ph]].
- [15] T. Lappi and R. Venugopalan, Phys. Rev. **C74**, 054905 (2006), [arXiv:nucl-th/0609021].
- [16] T. Hirano, U. W. Heinz, D. Kharzeev, R. Lacey and Y. Nara, Phys. Lett. **B636**, 299 (2006), [arXiv:nucl-th/0511046].
- [17] H.-J. Drescher and Y. Nara, Phys. Rev. **C76**, 041903 (2007), [arXiv:0707.0249 [nucl-th]].
- [18] T. Lappi, Phys. Rev. **C70**, 054905 (2004), [arXiv:hep-ph/0409328].
- [19] H. J. Drescher and Y. Nara, Phys. Rev. **C75**, 034905 (2007), [arXiv:nucl-th/0611017].
- [20] STAR, P. Sorensen, J. Phys. **G35**, 104102 (2008), [arXiv:0808.0356 [nucl-ex]]; PHOBOS, B. Alver *et al.*, J. Phys. **G35**, 104101 (2008), [arXiv:0804.4297 [nucl-ex]].
- [21] J. Putschke, J. Phys. **G34**, S679 (2007), [arXiv:nucl-ex/0701074]; STAR, M. Daugherty, arXiv:0806.2121 [nucl-ex]; STAR, B. K. Srivastava, Int. J. Mod. Phys. **E16**, 3371 (2008), [arXiv:nucl-ex/0702054].
- [22] STAR, S. A. Voloshin, arXiv:0806.0029 [nucl-ex].
- [23] A. Dumitru, F. Gelis, L. McLerran and R. Venugopalan, Nucl. Phys. **A810**, 91 (2008), [arXiv:0804.3858 [hep-ph]]; F. Gelis, T. Lappi and R. Venugopalan, arXiv:0810.4829 [hep-ph].
- [24] D. Kharzeev, A. Krasnitz and R. Venugopalan, Phys. Lett. **B545**, 298 (2002), [arXiv:hep-ph/0109253]; D. E. Kharzeev, L. D. McLerran and H. J. Warringa, Nucl. Phys. **A803**, 227 (2008), [arXiv:0711.0950 [hep-ph]].